Journal of Southeast University (English Edition) Vol. 39, No. 2, pp. 161 - 168 June 2023 ISSN 1003—7985

Inversion method for NMR weak signals with short relaxation time

Yu Qiaoming Lu Rongsheng Chen Lang Jiang Xiaowen
Wu Zhengxiu Bao Chong Ni Zhonghua

(Jiangsu Key Laboratory for Design and Manufacture of Micro-Nano Biomedical Instruments, Southeast University, Nanjing 211189, China)
(School of Mechanical Engineering, Southeast University, Nanjing 211189, China)
(National Key Laboratory of Bioelectronics, Southeast University, Nanjing 211189, China)

Abstract: An improved inversion method for nuclear magnetic resonance (NMR) relaxation signals with a low signal-to-noise ratio (SNR) is proposed to solve the inversion problem of weak NMR signals with short relaxation components. This method selects a suitable filter factor for inversion by combining the singular-value decomposition and Tikhonov methods. Compared with existing inversion methods, the relaxation-time spectrum based on the proposed method is closer to the original spectrum of the NMR simulation signal, especially in short relaxation components when the signal is weak. The reliability of the proposed method under different SNRs was proven by calculating the uncertainty of the solutions. The ability to obtain precise relaxation times was proven by experimental measurement and inversion analysis of samples with multiple relaxation components. The changing pattern of the components in a cement-hydration process found by identifying the weak signal with short relaxation components was validated. In conclusion, the proposed inversion method can effectively distinguish a weak NMR signal with short relaxation times, which plays an important role in determining the key components of a sample and in characterizing its physical properties, thus promoting the application of NMR relaxation technology.

Key words: nuclear magnetic resonance (NMR); relaxation time; inversion; low signal-to-noise ratio (SNR); cement hydration

DOI: 10.3969/j.issn.1003-7985.2023.02.007

The ^{1}HNuclear magnetic resonance (NMR) relaxation measurement is an essential non-invasive and nondestructive detection method that is widely used in physics, chemistry, biomedicine, and petroleum exploration. The physical properties of samples, such as the composition and pore-size distribution, can be characterized and quantified using the relaxation-time distribution obtained by inverse processing of NMR relaxation signals [1-5]. Further, the inversion of weak signals with short relaxation components, which play a decisive role in representing the characteristics of samples, has always been an intractable problem.

The inversion of an NMR signal is a typical ill-conditioned problem in which the principle requires solving the first Fredholm equation. Two main methods are available to solve this problem: one is the singular-value decomposition (SVD) algorithm, and the other is the regularization algorithm [6-7]. The SVD algorithm aims to reduce the ill condition of an inversion problem by truncating the smaller singular values in the coefficient matrix. The core of the regularization algorithm is the penalty term added to the original equation to suppress the instability of the solution. The regularization algorithms mainly include the Tikhonov regularization, CONTIN [8], L_1-norm [9], and hybrid L_1/L_2-norm algorithms [10]. The Tikhonov regularization algorithm is most commonly used in NMR owing to its simplicity in terms of mathematics. The weight of the objective function and penalty term is called a smooth factor, which keeps the solution between distortion and ill condition balanced. In addition, the suboptimal value of the smooth factor can be determined using the Butler-Reeds-Dawson [11] and L-curve algorithms [12]. Li et al. [13] proposed a random SVD (RSVD) method, which required lesser computing time and memory in large-scale matrix decomposition. Thus, RSVD could achieve high-resolution inversion of 2D and 3D NMRs with higher computational efficiency than SVD. Zou et al. [14] proposed a novel compression method that combined the advantages of window averaging and SVD methods, which achieved good application results in NMR data compression. In addition, improved methods based on the regularization method can be found in existing research. Guo et al. [15] chose a surrogate objective

Received 2022-08-12, **Revised** 2023-03-12.

Biographies: Yu Qiaoming (1997—), male, graduate; Lu Rongsheng (corresponding author), male, doctor, professor, lurs@seu.edu.cn.

Foundation items: The National Natural Science Foundation of China (No. 52075098), the National Key Scientific Instrument and Equipment Development Project of China (No. 51627808).

Citation: Yu Qiaoming, Lu Rongsheng, Chen Lang, et al. Inversion method for NMR weak signals with short relaxation time[J]. Journal of Southeast University (English Edition), 2023, 39(2): 161 - 168. DOI: 10.3969/j.issn.1003-7985.2023.02.007.

function that was based on least squares fitting to avoid the process of choosing a regularization parameter. Venkataramanan et al. [16] transformed the constrained optimization problem into an unconstrained optimization problem in a low-dimensional space whose dimension was determined by the number of significant singular values. Lu et al. [17] converted a minimum objective function with nonnegative constraints into an unconstrained maximization problem to reduce sensitivity to noise. In addition to the above-mentioned methods, some advanced algorithms are available, such as the Monte Carlo (MC) method [18] and genetic algorithms [19]. However, because of the complexity and time requirements for searching for the global optimal solution, they are not advantageous, especially in large-scale data processing, and cannot satisfy the requirements of real-time processing.

In summary, the disadvantage of the SVD algorithm comes from its difficulty in determining the position of truncation, which destroys the continuity of the spectrum, resulting in the loss of characteristic peaks of weak signals. Although the truncation value can be effectively determined by the signal-to-noise ratio (SNR), the inversion stability of the SVD algorithm in low SNR is not improved, and the inversion accuracy of a weak signal cannot be effectively guaranteed. With regard to the regularization method, searching for an appropriate smooth factor is difficult. In addition, the smooth factor causes opposite effects on short and long relaxation times, which leads to the overfitting of small peaks (short relaxation times) and underfitting of large peaks (long relaxation times) under the same smooth factor. In this paper, we propose an improved inverse method for the accurate identification of weak NMR short relaxation signals by combining the SVD and Tikhonov methods. The idea of this method is to select a more appropriate filter factor between the SVD and Tikhonov algorithms based on the singular value.

1 Inversion Method of Short Relaxation and Weak Signal in 1D NMR

The pulse sequences commonly used in 1D NMR relaxation measurements include the Carr-Purcell-Meiboom-Gill (CPMG), inversion-recovery, and saturation-recovery pulse sequences. The kernel matrix in the inversion algorithm must match the type of pulse to correctly separate the relaxation components. The CPMG pulse sequence was considered to illustrate the inversion method of 1D NMR. The measured echo amplitude decayed according to the sum of the exponential expansion as follows:

$$b_i = \sum f_j \exp\left(-\frac{t_i}{T_{2j}}\right) + \varepsilon_i \tag{1}$$

where b_i is the echo-amplitude value at t_i; T_{2j} is the relaxation time of the j component whose interval porosity is f_j; t_i is an integer multiple of the time of echo (T_E), which is equal to (iT_E); ε_i is the stochastic white noise that obeys a Gauss distribution[19]. When the sample consists of n components and m echo points are collected, Eq. (1) can be rewritten in a matrix form as follows:

$$\boldsymbol{b} = \boldsymbol{K}\boldsymbol{f} + \boldsymbol{\varepsilon} \tag{2}$$

where $\boldsymbol{b} \in \mathbf{R}^m$, $\boldsymbol{K} \in \mathbf{R}^{m \times n}$, and $\boldsymbol{f} \in \mathbf{R}^n$. We note that the elements of density function f must be nonnegative because they represent the proportion that each component contributes to the whole echo amplitude. The inversion process estimates density function $\boldsymbol{f}$ from measured data m under the condition of non-nonnegative constraints. The solution of Eq. (2) can be expressed as

$$\arg\min_{f \geqslant 0} = \left\| \boldsymbol{K}\boldsymbol{f} - \boldsymbol{m} \right\|^2 \tag{3}$$

Inversion is an ill-conditioned problem, which means that a small perturbation in the solution can lead to a large variation in the final solution. The existing inversion methods suffer from limitations in dealing with weak signals. However, the improved method combines the SVD and regularization methods by analyzing their filter factors; thus, the superior filter factor is automatically adopted with the change in the singular value.

1.1 SVD and Tikhonov regularization algorithm

According to the SVD theory, $\boldsymbol{K}_{m \times n}$ can be decomposed into the product of orthogonal matrix $\boldsymbol{U}_{m \times m} = [\boldsymbol{u}_1 \ \boldsymbol{u}_2 \ \cdots \ \boldsymbol{u}_m]$, $\boldsymbol{V}_{n \times n} = [\boldsymbol{v}_1 \ \boldsymbol{v}_2 \ \cdots \ \boldsymbol{v}_n]$, and nonnegative diagonal matrix $\boldsymbol{\Sigma}_{\times r} = \mathrm{diag}(s_1, s_2, \ldots, s_r)$. It can be expressed as

$$\boldsymbol{K}_{m \times n} = \boldsymbol{U}_{m \times m} \begin{bmatrix} \boldsymbol{\Sigma}_{\times r} & \boldsymbol{0} \\ \boldsymbol{0} & \boldsymbol{0} \end{bmatrix}_{m \times n} \boldsymbol{V}^{\mathrm{T}}_{n \times n} \tag{4}$$

where r is the rank of $\boldsymbol{K}_{m \times n}$; s_i represents the singular values of $\boldsymbol{K}_{m \times n}$, which decreases with i[20]. Thus, the solution of Eq. (3) can be expressed as [21]

$$\boldsymbol{s}_{\mathrm{LSM}} = \boldsymbol{K}^{+}\boldsymbol{b} = \sum_{i=0}^{r} \frac{\boldsymbol{u}_i^{\mathrm{T}}\boldsymbol{b}}{s_i} \boldsymbol{v}_i \tag{5}$$

where $\boldsymbol{K}^{+}$ is the generalized inverse matrix of $\boldsymbol{K}$.

Eq. (5) shows that the deviation of the solution is greatly amplified by the near-zero singular values, which undermines the reliability of the inversion results. Thus, the main idea of SVD is to truncate the singular values to obtain a stable and credible solution. In addition, the solution of Eq. (3) in the SVD method is expressed as

$$\boldsymbol{f}_{\mathrm{SVD}} = \sum_{i=0}^{k} \frac{\boldsymbol{u}_i^{\mathrm{T}}\boldsymbol{b}}{s_i} \boldsymbol{v}_i \tag{6}$$

Eq. (6) shows that the first k singular values are retained and the remaining values are set to zero. Value k is mostly determined by the SNR and condition number, which decide the fidelity of the SVD method. An inappropriate truncated position can cause a serious loss in the spectral components.

The idea of the Tikhonov regularization method is to add a penalty term based on the least square criterion. It converts the inversion problem into the following:

$$\arg\min_{f\geqslant 0} = \|\boldsymbol{Kf}-\boldsymbol{b}\|^2 + \alpha^2\|\boldsymbol{Lf}\|^2 \tag{7}$$

where $\|\boldsymbol{Kf}-\boldsymbol{b}\|^2$ is the residual and $\|\boldsymbol{Lf}\|^2$ is the smooth function; α is the smooth factor that keeps the balance between the residual and smooth function; matrix $\boldsymbol{L}$ is called the regularization matrix, which can be a derivative operator of the zeroth, first, or second order, representing the modular, curvature, or slope smoothness of the solution, respectively. Eq. (7) is called the standard Tikhonov regularization when matrix $\boldsymbol{L}$ is an identity matrix. The solution of Eq. (7) can be expressed as

$$\boldsymbol{f}_{\mathrm{Tik}} = \sum_{i=0}^{n} \frac{s_i^2}{s_i^2+\alpha^2}\frac{\boldsymbol{u}_i^{\mathrm{T}}\boldsymbol{b}}{s_i}\boldsymbol{v}_i \tag{8}$$

1.2 Filter-factor fusion method

The principle of all the methods in solving the inverse problem is the modification of the least square method, which adds filter factors to reduce the noise effect. According to Eqs. (5), (6), and (8), the filter factors of the SVD and Tikhonov methods are

$$F_{\mathrm{SVD}} = \begin{cases} 1 & i\leqslant k \\ 0 & \text{otherwise} \end{cases}, \quad F_{\mathrm{Tik}} = \frac{s_i^2}{s_i^2+\alpha^2} \tag{9}$$

For SVD, the small singular value of $\boldsymbol{K}$ and the corresponding eigenvector are eliminated to improve the inversion stability. Although it ameliorates the ill-conditioned problem, many components in the NMR spectra are left out, leading to serious distortion in the inversion when k is small. In addition, the Tikhonov regularized filter factor introduces a large effect on the correction of singular values, which affects the inversion accuracy. Thus, the solution is modified by combining the filter factors of the SVD and Tikhonov methods and is expressed as

$$\boldsymbol{f}_{\mathrm{impr}} = \sum_{i=0}^{n} F_i\frac{\boldsymbol{u}_i^{\mathrm{T}}\boldsymbol{b}}{s_i}\boldsymbol{v}_i$$

$$F_i = \begin{cases} 1 & i\leqslant k \\ \dfrac{s_i^2}{s_i^2+\alpha^2} & \text{otherwise} \end{cases} \tag{10}$$

To solve Eq. (10), boundary value k must first be confirmed, which is similar to the truncation position-determination method of the SVD method. The general principle of determination is to retain as many original singular values as possible on the basis of ensuring the stability of the equation. The method adopted in this study makes the reserved singular value greater than the ratio of the maximum singular value and SNR. The value of smooth factor α is determined using the L-curve method.

The algorithm execution flow of the inversion method proposed in this paper is described as follows:

1) The distribution of T_2 is set, and the coefficient matrix $\boldsymbol{K}$ is solved.

2) Initial solution $\boldsymbol{s}^*$ and convergence tolerance ε are solved.

3) Residual $\Delta\boldsymbol{m} = \boldsymbol{m} - \boldsymbol{K}\boldsymbol{s}^*$ is calculated.

4) Residual $\Delta\boldsymbol{s}$ is calculated from $\Delta\boldsymbol{m} = \boldsymbol{K}\Delta\boldsymbol{s}$.

5) Solution $\boldsymbol{s}^* = \boldsymbol{s}^* + \Delta\boldsymbol{s}$ is updated.

6) If $\|\Delta\boldsymbol{s}\| < \varepsilon$, then $\boldsymbol{s}^*$ is the optimal solution; otherwise, Steps 3) to 5) are repeated.

2 Experiments and Results

2.1 Numerical simulation

The NMR transverse relaxation time (T_2) of liquid (e.g., oil and water) greatly changed in different pore structures. Thus, we constructed two typical oil-water bimodal T_2 distribution models: Models A and B. T_2 of oil was 200 ms in both models, and T_2 of water was 15 ms in Model A and 2 ms in Model B. Model A is shown in Fig. 1, and Model B is shown in Fig. 2 The peaks represent

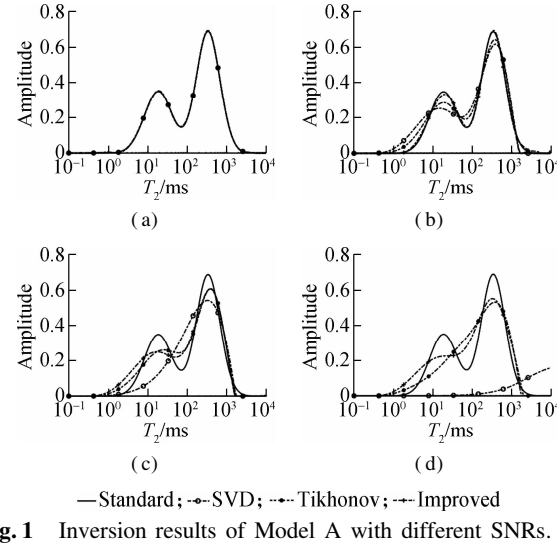

Fig. 1 Inversion results of Model A with different SNRs. (a) 80 dB; (b) 40 dB; (c) 20 dB; (d) 10 dB

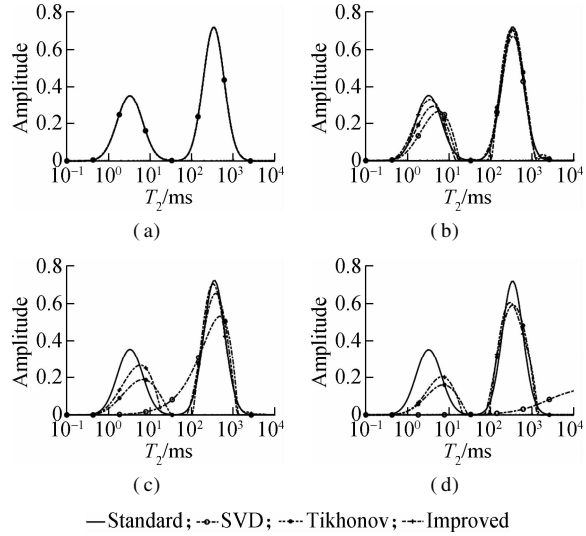

Fig. 2 Inversion results of Model B with different SNRs. (a) 80 dB; (b) 40 dB; (c) 20 dB; (d) 10 dB

the types of components, and the height of the peak indicates the weight of the component in the total signal. Model A, whose two peaks partly overlapped, and Model B, whose two peaks were separated, are the most common models used in practice. In the numerical simulation, the value of T_2 was logarithmically discretized with 64 points that ranged from 0.1 to 10 000 ms. The original signals were collected from 1 000 echoes with the time of echo being 0.5 ms. Gaussian noises at different levels were added to the original signals to create NMR signals with SNRs of 80, 40, 20, and 10 dB.

Before the inversion operation was performed, the SVD method was employed to compress the NMR signals to improve the inversion efficiency. Then, we compared the improved algorithm with the Tikhonov and SVD algorithms by inverting the echo signals with different SNRs.

For Model A shown in Fig. 1, the results from the three methods were identical to the original NMR T_2 distribution when SNR is 80 dB. However, the inversion result deviated from the real curve with the increase in noise. The left peak of Model A was seriously disturbed due to its short T_2 and small semaphore when the SNR was lower than 40 dB, and its value exhibited a gradual decrease. The bimodal distribution of T_2 in the Tikhonov and SVD algorithms coalesced into one peak at a low SNR level. The number of singular values omitted in the SVD algorithm was large when the SNR was less than 10 dB, and it seriously damaged the accuracy of the inversion result and caused the loss of characteristic information of the original peaks. In addition, the Tikhonov algorithm without truncation of the singular values performed better than the SVD method at low SNR. The improved method truncated the larger singular values and modified the smaller singular values, which assimilated the advantages of the SVD and Tikhonov methods.

For Model B shown in Fig. 2, the two characteristic peaks could be clearly recognized when SNR was high. When SNR was lower than 40 dB, a significant drop in the characteristic peaks and an obvious shift in the short relaxation peak to the right occurred. By comparing the inversion results of the three methods based on the two general models, the effectiveness and reliability of the improved inversion method in the case of low SNR were fully demonstrated.

The deviation between the solution obtained by the improved algorithm and the true value was less than 20% when SNR is 4 dB in Model A or 6 dB in Model B. However, the solution calculated by the Tikhonov method exhibited three peaks, and the solution obtained by the SVD method had no visible peak. Compared with the Tikhonov and SVD methods, the relative error in the short relaxation part could be reduced by 8.9% to 21% below 40 dB using the improved method, which demonstrated the effectiveness of the improved method at low SNR, and short relaxation was demonstrated.

The performance under different SNRs of the improved method could be determined based on the coincidence between the confidence interval of the solution and the true curve. A method to calculate the confidence interval was proposed by Prange et al. [22] using enhanced Gibbs sampling to generate a large number of T_2 spectra according to Bayesian inference. The noise in the T_2 signals often presents an uncorrelated normal distribution [23]. Further, the uncertainty of T_2 could be calculated using the truncated multivariate normal distribution, as expressed in the following equation:

$$\pi(\boldsymbol{f}) = \exp\left[-\frac{1}{2}(\boldsymbol{b}-\boldsymbol{K}\boldsymbol{f})^{\mathrm{T}}\boldsymbol{\Lambda}^{-1}(\boldsymbol{b}-\boldsymbol{K}\boldsymbol{f}) \right] \qquad \boldsymbol{f}\geqslant 0 \tag{11}$$

where $\boldsymbol{b}$ is the collected signal; $\boldsymbol{f}$ is the distribution spectrum to be calculated; $\boldsymbol{K}$ is the kernel matrix with elements $k_{ij} = \exp(-t_i/T_{2j})$; and $\pi(\boldsymbol{f})$ is the probability density function of $\boldsymbol{f}$. $\boldsymbol{\Lambda}$ represents a diagonal matrix containing the noise variance versus time, which is always expressed as $\sigma^2\boldsymbol{I}$, where σ is the measured noise variance and $\boldsymbol{I}$ is the identity matrix.

According to the MC method, the characteristics of a system can be obtained through a large number of random samples. The uncertainty calculation of the solution was transformed into a collection of a huge number of truncated multivariate normal-distribution samples from Eq. (11). The 2D slice sampler proposed by Philippe could sample from the truncated multinormal distribution expressed in Eq. (11) in high dimensions using the inversion curve and covariance matrix [24]. The inversion curve represented the inversion solution generated by the improved method, and the covariance matrix could be expressed as $(\sigma^{-2}\boldsymbol{K}^{\mathrm{T}}\boldsymbol{K})^{-1}$. Thus, the uncertainty of the T_2 spectra could be obtained from the statistical properties of the samples drawn from $\pi(\boldsymbol{f})$ without a complex formula.

The T_2 spectrum model with bimodal T_2 shown in Fig. 3 represented the above mentioned Model A. We drew 10 000 samples from the data in Model A, and every sample could be considered a potential solution to the Fredholm integral equation. Then, the uncertainty of T_2 could be calculated by performing mathematical statistics on a large number of samples. The mean T_2 spectrum was computed from 10 000 samples for the data in Model A, and the confidence interval represented the mean plus or minus one standard deviation. Fig. 3 shows that the confidence interval was narrow at high SNR with little deviation from the original data, which satisfied the expectation. The width of the confidence interval and the degree of deviation increased as SNR decreased. The confidence interval composed of one standard deviation could contain almost all the original data even in very low SNR, which proved the reliability and availability of the inversion

spectra inverted by the improved inversion method. According to the physical significance of f, the samples were non-negative constrained, which forced their mean value to be positive and generated an upward deviation of the confidence interval.

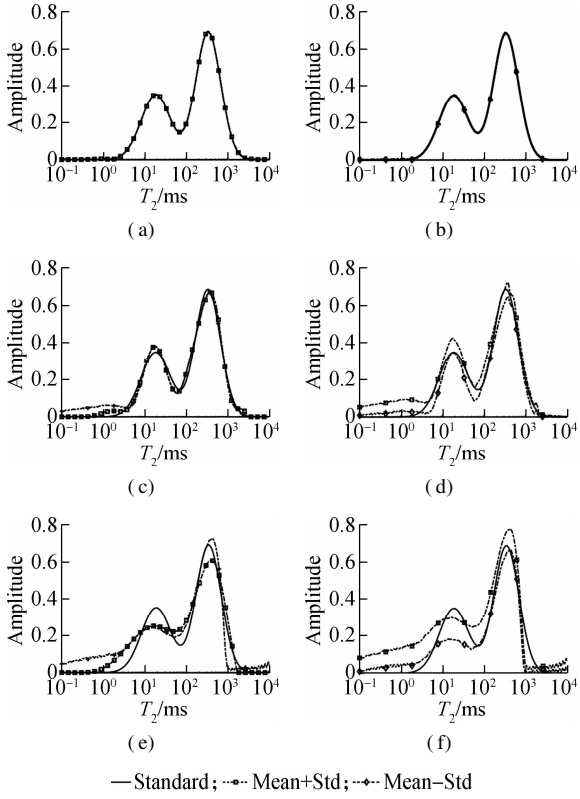

Fig. 3 Uncertainty of T_2 obtained by the improved method at different SNRs. (a) Mean at 80 dB; (b) Confidence interval at 80 dB; (c) Mean at 40 dB; (d) Confidence interval at 40 dB; (e) Mean at 20 dB; (f) Confidence interval at 20 dB

2.2 Inversion of the standard sample signal

The NMR T_2 distributions varied with the concentrations of $CuSO_4 \cdot 5H_2O$ solutions. The NMR signals obtained through sealing and introducing $CuSO_4 \cdot 5H_2O$ solutions in one probe represented the superposition of NMR signals of $CuSO_4 \cdot 5H_2O$ solutions in various concentrations. Three groups of samples were used in the experiment, and each group was composed of three concentrations of $CuSO_4 \cdot 5H_2O$ solution. The T_2 types of each component were denoted as T_{21}, T_{22}, and T_{23}. The NMR signal was detected using a low-field NMR instrument independently developed in the laboratory. In the experiment, the scanning times were four, the measurement time was 500 ms, and the number of collected points was 2 048.

The T_2 distributions of the three types of standard samples obtained by the improved, SVD, and Tikhonov methods are shown in Fig. 4. Three inversion peaks were obtained by all methods. In the NMR inversion, the smoothness of the peak indicated that several components with similar relaxation times existed nearby, whereas the composition near the steep peaks was relatively alone. By comparing the mentioned inversion methods, the T_2 distribution obtained by the improved method exhibited three steeper and clearer peaks, which was consistent with the actual condition of the standard sample. In addition, the accuracy of the improved method in multicomponent inversion was verified by the atlas, where the abscissa of each peak obtained by the improved method was closer to that of the standard samples.

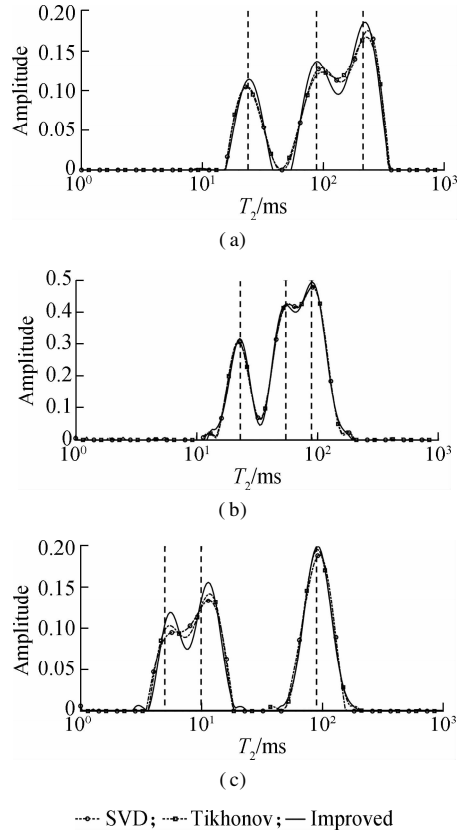

Fig. 4 Inversion results of the NMR signals of three different standard samples. (a) Group 1; (b) Group 2; (c) Group 3

Tab. 1 lists the specific values of T_2 for each component in the standard sample that were configured and compared with the standard T_2 values. According to Tab. 1, the relative error between the estimated and standard values of T_2 was minimum, which objectively confirmed the accuracy of the inversion method proposed in this paper.

2.3 Signal inversion of the cement-hydration process

The transformation of the pore size and the pattern of water migration during cement hydration are very important for the research on the mechanical properties of cement materials. The improved method was applied to identify the variation in the pore size and content of the interlayer water, gel water, and capillary water during the hydration and maturation of cement samples, which are correlated with T_2, as well as the process of capillary-water migration to other pores.

Tab. 1 Comparison of the inversion results of the standard samples from different inversion methods

Sample	Method	T_{21}/ms	T_{21} relative error/%	T_{22}/ms	T_{22} relative error/%	T_{23}/ms	T_{23} relative error/%
1	Standard	210.0		90.0		24.0	
	SVD	213.4	1.62	90.9	1.00	22.5	6.25
	Tikhonov	212.1	1.00	88.7	1.44	23.2	3.33
	Improved	209.4	0.29	91.0	1.11	24.3	1.25
2	Standard	90.0		55.0		24.0	
	SVD	90.4	0.44	54.8	0.36	24.5	2.08
	Tikhonov	90.1	0.11	54.6	0.73	24.2	0.83
	Improved	90.2	0.22	55.0	0	24.1	0.42
3	Standard	90.0		10.0		5.0	
	SVD	91.4	1.56	11.9	19.00	5.2	4.00
	Tikhonov	91.1	1.22	12.9	29.00	5.3	6.00
	Improved	90.4	0.44	11.1	11.00	5.0	0

The low-field NMR instrument used in the experiment was independently developed in our laboratory. The instrument consists of a permanent magnet for generating a static main magnetic field (0.5 T field intensity), a probe for transmitting radio-frequency (RF) field and receiving NMR signal (diameter 30 mm and probe death time 15 μs), and an electronic control system for generating pulse signal and processing nuclear magnetic resonance signal (RF amplifier power 250 W).

The cement used in the experiment was white cement with a water-cement ratio of 0.4 and a height of 30 mm, which was sealed in a glass tube with a diameter of 30 mm to prevent the evaporation of water in the cement. The NMR relaxation signals in the cement samples were mainly derived from various bound-water signals. The state of moisture and the pore-size information in the cement were reflected using the discrepancy in the transverse relaxation time of the bound water. For instance, the minimum relaxation time of the interlayer water was only tens of microseconds with weak signal intensity, which is a typical sample with a short relaxation time.

The NMR transverse relaxation-time distributions obtained by the SVD and improved methods at different stages of cement hydration are shown in Fig. 5. The improved method inverted a more valuable atlas that showed distinguishable peaks, whereas the SVD method failed to clearly identify the type of bound water in this experiment. According to the transverse relaxation time and cement composition, the left peak signifies the signal of interlayer water, the middle peak denotes the signal of gel water, and the right peak represents the signal of capillary water. From the change in the transverse relaxation time in the cement-hydration process, the transverse relaxation time of the capillary and gel water gradually shifted to the left with the increase in the cement setting time, whereas that of the interlayer water tended to be stable after one day. From the height variation of the peak in the inversion map, the content of capillary water decreased with the increase in time, and that of gel water

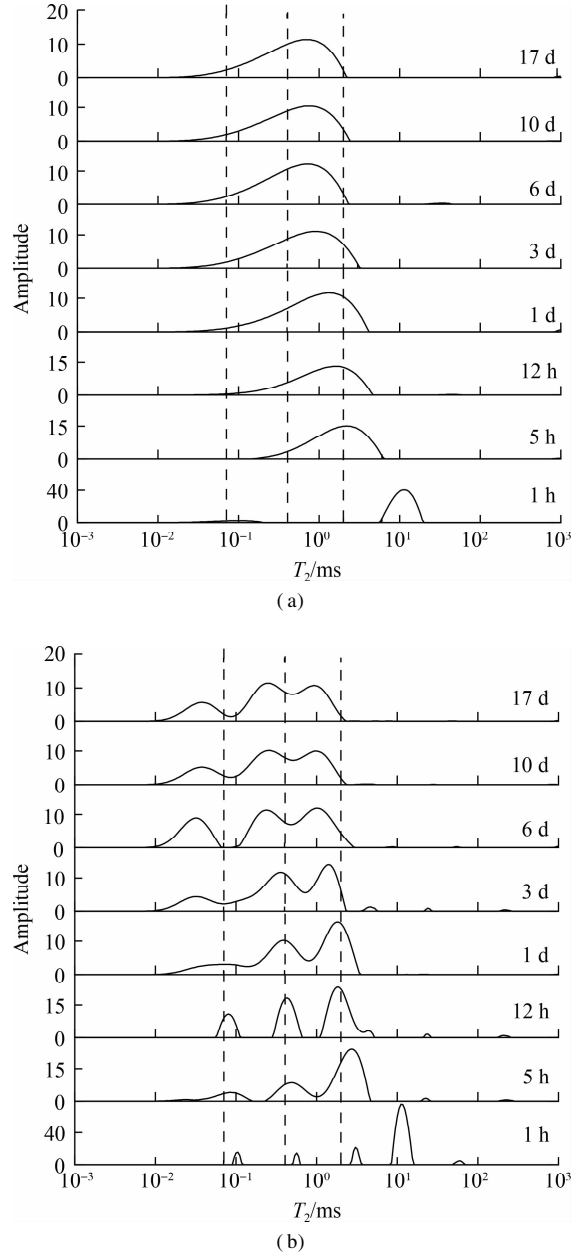

Fig. 5 Distribution of T_2 different periods in the cement-hydration process. (a) SVD method; (b) Improved method

increased with little change in the content of interlayer water. These trends were also consistent with the cement-hydration process mentioned in Ref. [25], which effectively explained the correctness of the inversion method in practical applications.

3 Conclusions

1) Compared with the SVD and Tikhonov methods, the proposed method leads to more accurate results in low SNRs, which is crucial for the precise identification of unknown weak components in samples.

2) The experimental results show that the component types of the sample identified by the proposed method are more accurate. In addition, the T_2 value estimated in each component is closest to the standard value with a small relative error, which proves the correctness and accuracy of the proposed method in the multicomponent sample signal inversion.

3) The proposed method is applied to identify the variation trend of each component in the hydration process of cement samples. Further, the changes in the peaks with the increase in the cement curing time corresponding to the interlayer, gel-pore, and capillary water are consistent with the conclusion in the relevant literature on cement research.

4) The proposed method realizes the inversion of NMR signals with multicomponent samples at low SNRs and correctly and accurately identifies the weak signals with short relaxation components, which plays an important role in the discovery of key components in the samples and the characterization of their physical properties. It also promotes the wide application of low-field NMR relaxation techniques.

References

[1] Bilaniuk L T, Bilaniuk O M. NMR imaging in medicine [J]. *Physics Education*, 1984, **19**(5): 247 − 252.

[2] Gambhir P N. Applications of low-resolution pulsed NMR to the determination of oil and moisture in oilseeds [J]. *Trends in Food Science & Technology*, 1992, **3**: 191 − 196. DOI: 10.1016/0924-2244(92)90188-3.

[3] Price W S, Ide H, Arata Y. Self-diffusion of supercooled water to 238 K using PGSE NMR diffusion measurements[J]. *Journal of Physical Chemistry A*, 1999, **103**: 448 − 450. DOI: 10.1021/JP9839044.

[4] Herzfeld J, Berger A E. Sideband intensities in NMR spectra of samples spinning at the magic angle[J]. *The Journal of Chemical Physics*, 1980, **73**(12): 6021 − 6030. DOI: 10.1063/1.440136.

[5] Han Y J, Zhou C C, Fan Y R, et al. A new permeability calculation method using nuclear magnetic resonance logging based on pore sizes: A case study of bioclastic limestone reservoirs in the A oilfield of the Mid-East[J]. *Petroleum Exploration and Development*, 2018, **45**(1): 183 − 192. DOI: 10.1016/S1876-3804(18)30019-3.

[6] Gao Y, Xiao L Z, Wu B S. TSVD and Tikhonov methods and influence factor analysis for NMR data in shale rock[J]. *Journal of Petroleum Science and Engineering*, 2020, **194**: 107508. DOI: 10.1016/j.petrol.2020.107508.

[7] Chen L. *Accurate inversion algorithm of low-field nuclear magnetic resonance signal and development of its software platform* [D]. Nanjing: Southeast University, 2020. (in Chinese)

[8] Provencher S W. CONTIN: A general purpose constrained regularization program for inverting noisy linear algebraic and integral equations[J]. *Computer Physics Communications*, 1982, **27**(3): 229 − 242. DOI: 10.1016/0010-4655(82)90174-6.

[9] Zhou X L, Su G Q, Wang L J, et al. The inversion of 2D NMR relaxometry data using L1 regularization[J]. *Journal of Magnetic Resonance*, 2017, **275**: 46 − 54. DOI: 10.1016/j.jmr.2016.12.003.

[10] Zou Y L, Xie R H, Liu M, et al. Nuclear magnetic resonance spectrum inversion based on the residual hybrid l_1/l_2 norm[J]. *IEEE Geoscience and Remote Sensing Letters*, 2018, **15**(8): 1194 − 1198. DOI: 10.1109/LGRS.2018.2835457.

[11] Butler J P, Reeds J A, Dawson S V. Estimating solutions of first kind integral equations with nonnegative constraints and optimal smoothing[J]. *SIAM Journal on Numerical Analysis*, 2006, **18**(3): 381 − 397.

[12] Hansen P C. Analysis of discrete ill-posed problems by means of the L-curve[J]. *SIAM Review*, 1992, **34**(4): 561 − 580. DOI: 10.1137/1034115.

[13] Li H T, Hu X F, Deng S G, et al. Fast multidimensional NMR inversion based on randomized singular value decomposition[J]. *Journal of Petroleum Science and Engineering*, 2020, **190**: 107044. DOI: 10.1016/j.petrol.2020.107044.

[14] Zou Y L, Xie R H. A novel method for NMR data compression[J]. *Computational Geosciences*, 2015, **19**(2): 389 − 401. DOI: 10.1007/s10596-015-9479-6.

[15] Guo J F, Xie R H. An inversion of NMR echo data based on a normalized iterative hard thresholding algorithm[J]. *IEEE Geoscience and Remote Sensing Letters*, 2018, **15**(9): 1332 − 1336. DOI: 10.1109/LGRS.2018.2844411.

[16] Venkataramanan L, Song Y Q, Hurlimann M D. Solving Fredholm integrals of the first kind with tensor product structure in 2 and 2.5 dimensions[J]. *IEEE Transactions on Signal Processing*, 2002, **50**(5): 1017 − 1026. DOI: 10.1109/78.995059.

[17] Lu R S, Bao C, Chen L, et al. A novel inversion method of 2D TD-NMR signals based on realizing unconstrained maximization of objective function[J]. *Journal of Magnetic Resonance*, 2022, **337**: 107168. DOI: 10.1016/j.jmr.2022.107168.

[18] Salazar-Tio R, Sun B Q. Monte Carlo optimization-in-

version methods for NMR[J]. *Petrophysics*, 2010, **51**(3): 208-218.

[19] Maojin T A N, Yaolin S H I, Guanbao X I E. NMR T2 distribution inversion based on genetic algorithm[J]. *Well Logging Technology*, 2007, **31**(5): 413-416.

[20] Prammer M G. NMR pore size distributions and permeability at the well site[C]//*SPE Annual Technical Conference and Exhibition*. New Orleans, LA, USA, 1994: 55-64. DOI: 10.2118/28368-MS.

[21] Guo S M, Li H, Guo J. A new Tikhonov regularization method[J]. *Journal of Southwest China Normal University* (*Natural Science Edition*), 2018, **43**(6): 46-51. DOI: 10.13718/j.cnki.xsxb.2018.06.009. (in Chinese)

[22] Prange M, Song Y Q. Quantifying uncertainty in NMR T2 spectra using Monte Carlo inversion[J]. *Journal of Magnetic Resonance*, 2009, **196**(1): 54-60. DOI: 10.1016/j.jmr.2008.10.008.

[23] Prange M, Song Y Q. Understanding NMR T(2) spectral uncertainty[J]. *Journal of Magnetic Resonance*, 2010, **204**(1): 118-123. DOI: 10.1016/j.jmr.2010.02.010.

[24] Philippe A, Robert C P. Perfect simulation of positive Gaussian distributions[J]. *Statistics and Computing*, 2003, **13**(2): 179-186. DOI: 10.1023/A:1023264710933.

[25] Muller A C A. *Characterization of porosity & C-S-H in cement pastes by* ^{1}H *NMR*[D]. Lausanne, Switzerland: EPFL, 2014.

一种面向核磁共振短弛豫弱信号的反演方法

余樵铭　陆荣生　陈　朗　姜晓文　吴正秀　鲍　冲　倪中华

(东南大学江苏省微纳生物医疗器械设计与制造重点实验室,南京 211189)
(东南大学机械工程学院,南京 211189)
(东南大学生物电子学国家重点实验室,南京 211189)

摘要:针对具有短弛豫分量的核磁共振弱信号的反演难题,提出了一种适用于低信噪比核磁共振弛豫信号的反演方法,通过结合 SVD 方法和 Tikhonov 方法,选择更加合适的滤波因子进行反演.与现有的反演方法相比,该方法获得的弛豫时间分布图谱更接近于核磁共振模拟信号的原始谱,尤其是信号较弱时的短弛豫分量.通过计算反演结果的不确定度,证明了该方法在不同信噪比下的可靠性.此外,通过实验测量和多弛豫分量样品的反演分析,表明该方法能够获得精确的弛豫时间.最后,将该方法应用于水泥水化过程核磁共振弛豫信号的分析,通过对短弛豫弱信号的有效辨识,准确发现了水泥水化过程中各组分的变化规律.证明了该方法能够有效分辨弛豫时间较短的核磁共振弱信号,对寻找样品关键成分和表征其物理性质具有重要作用,从而促进了核磁共振弛豫技术的应用.

关键词:核磁共振;弛豫时间;反演;低信噪比; 水泥水化

中图分类号:TH89